An Experimental Evaluation Based on Direction Finding Specification for Indoor Localization and Proximity Detection

Michele Girolami, Fabio Mavilia, Francesco Furfari, and Paolo Barsocchi

***Abstract*—Radio-frequency technologies have been largely explored to deliver reliable indoor localization systems. However, at the current stage, none of the proposed technologies represent a de-facto standard. Although RSS-based (received signal strength) techniques have been extensively studied, they suffer of a number of side-effects mainly caused by the complexity of radio propagation in indoor environments. A possible solution is designing systems exploiting multiple techniques, so that to compensate weaknesses of a specific source of information. Under this respect, Bluetooth represents an interesting technology, combining multiple techniques for indoor localization. In particular, the BT5.1 direction finding specification includes the possibility of estimating the angle between an emitting device and an antenna array. The Angle of Arrival (AoA) provides interesting features for the localization purpose, as it allows estimating the direction from which a signal is propagated. In this work, we detail our experimental setting based on a BT5.1-compliant kit to quantitatively measure the performance in three scenarios: static positioning, mobility, and proximity detection. Scenarios provide a robust benchmark allowing us to identify and discuss features of AoA values also in comparison with respect to traditional RSS-based approaches.**

***Index Terms*—Angle of arrival (AoA), Bluetooth 5.1, direction finding, indoor localization, proximity.**

I. Introduction

INDOOR positioning techniques and technologies have been radically changing the performance of systems designed to estimate the position of targets in indoor environments [1]. In the last ten years, technological trends clearly show the use of multiple sensing units to estimate the position or the proximity of a target with respect to a point of interest [2]. Under this respect, radio-frequency (RF) techniques largely exploit the analysis of the received signal strength (RSS) as it represents a key-metric to estimate the distance between an emitter and a receiver. Most of the proposed solutions rely on the correlation between the signal strength and the distance. In turn, the estimated distance can be used to localize a target with, e.g., a trilateration method. However, as shown by many results in the current literature [3], [4], RSS-based solutions suffer from a number of side-effects reducing the accuracy and the reliability with real-world experimental settings. Among them, we cite the multipath fading effect, the signal attenuation and the channel hopping. Received signal strength indicator (RSSI) values of advertising channels considerably differ from each other, causing a possible increase of the localization error [5]. Not only, but also the device heterogeneity further affects the performance. Indeed, the estimated RSSI of messages received from different devices might remarkably vary, due to the device's chipsets differ among the vendors or depleting batteries. As a result, localization systems based on a specific calibration device, might provide inaccurate results when changing the device. This is the case of the fingerprint [6] technique, which requires a device-based calibration phase to map the RSSI expected from each transmitter for every possible position of a mobile receiver in a space.

Recently, the Bluetooth Core Specification 5.1 provided by Bluetooth Special Interest Group (SIG) added direction finding (DF) feature in the low energy (LE) standard by modifying the packet structure in LE physical layer. The DF specification is targeted to indoor positioning [7], and it is based on Angle of Departure (AoD) and Angle of Arrival (AoA) techniques. The core idea is to estimate the angle between the emitting and the receiving device. To this purpose, the receiving device is equipped with an antenna array, used to measure the phase delay at multiple antennas. When multiple receiving devices estimate the corresponding AoAs for a target, then it is possible to localize it with a triangulation system. AoA computation requires a specific hardware, i.e., a receiving device equipped with multiple antennas. Moreover, the location of the anchor nodes represents a crucial aspect, to guarantee a certain degree of accuracy of the estimated AoA values. In fact, small variations of anchor's orientation might introduce a consistent error during the localization process. Nevertheless, according to our experimental tests, the estimated AoA values are less prone to significant fluctuations such as RSS at stationary conditions.

In this article, we detail our experimental campaign and the resulting performance. To this purpose, we adopt a BT5.1-compliant hardware kit, namely the XPLR-AOA by u-Blox. We identify three application scenarios: static positioning, mobility,

Manuscript received 13 November 2023; revised 4 December 2023; accepted 18 December 2023. Date of publication 20 December 2023; date of current version 5 January 2024. This work was supported in part by European Union - Next Generation EU, in the context of The National Recovery and Resilience Plan, Investment Partenariato Esteso PE8 "Conseguenze e sfide dell'invecchiamento", Project Age-IT, CUP: B83C22004800006. *(Corresponding author: Fabio Mavilia.)*

The authors are with the Institute of Information Science and Technologies, National Research Council, 56124 Pisa, Italy (e-mail: michele.girolami@isti.cnr.it; fabio.mavilia@isti.cnr.it; francesco.furfari@isti.cnr.it; paolo.barsocchi@isti.cnr.it).

Digital Object Identifier 10.1109/JISPIN.2023.3345268

and proximity. These scenarios cover complementary aspects of indoor localization, allowing us to stress the system at very different conditions. Concerning the static positioning scenario, we compute the localization error obtained from 28 reference locations. We also study the performance by varying the orientation of the target: North, East, West, and South. Concerning the mobility scenario, we compute the 75th percentile of the localization error in an indoor path. We show how errors are distributed in the reference environment. Finally, concerning the proximity scenario, our goal is detecting proximity or non-proximity events between two people approaching or moving away. Under this respect, we adopt state-of-the-art metrics assessing the performance of classification algorithms, such as the accuracy, precision, recall, and F-Score metrics. The adopted hardware estimates the AoA with two different angles, azimuth and elevation. With all the testing scenarios, the anchor node is always deployed on the ceiling of a wide indoor room. Bluetooth tags emit beacons based on the EddyStone frame at 50 Hz advertisement frequency. The collected dataset includes a timestamp followed by AoA values (azimuth and elevation), the RSSI and the Bluetooth channel used for the message propagation. From our experimental results, the static positioning scenario provides errors ranging from 1.82 to 1.90 m, while for the mobility scenario, the 75th percentile is 2.78 m. Concerning the proximity scenario, our algorithm correctly identifies the proximity with an accuracy score of 93%.

Beyond the results for the three scenarios, in this article we also analyze the distribution of the RSSI and of the AoA according to two features: The impact of the Bluetooth advertisement channels (channel 37, 38, and 39) and the influence of the target's orientation.

It is worth mentioning that this work introduces some relevant novelties not present in the current literature. They can be summarized as follows.

1) We outline an experimental setup tailored to assess the efficacy of indoor localization systems, leveraging a promising technique known as AoA. While AoA has been utilized in various application scenarios, its integration with Bluetooth technology has become available only in recent years. The chosen kit, the XPLR-AOA by u-Blox, provides us with the capability to gather estimated angles on two planes (azimuth and elevation), along with RSSI values. The fusion of RSSI and AoA enables a comprehensive study and comparison of these techniques for localization purposes.
2) The collected data have been analyzed through two innovative perspectives: the influence of Bluetooth channels and the influence of human posture. Both channel selection and posture significantly contribute to the overall outcomes. This study addresses these aspects explicitly, presenting clear and discernible results.
3) We replicate three distinct scenarios for indoor localization. Specifically, we gather data in static, mobile, and proximity scenarios, aiming to assess the performance of the adopted hardware under varying conditions of increasing complexity.

The rest of this article is organized as follows. Section II frames the state-of-the-art of indoor localization systems based on AoA. We explore the current literature to identify radio technologies, signal metrics, and positioning methods for indoor localization. In Section II, we also summarize works adopting a similar approach and we compare some distinguishing features. Section III details the DF specification and how AoA and AoD can be estimated with an antenna array. Section IV reports the data analysis for the static positioning scenario, while Section V provides the experimental results. Finally, Section VI concludes this article.

II. Related Work

Knowledge concerning the user's position in indoor environments represents a piece of key-context information in pervasive computing scenarios. During the last 15 years, many technologies and techniques have been adopted to localize a target. Nevertheless, those techniques based on RF have been gaining an increasing attention, due to the pervasive, personal, and ubiquitous features of mobile devices often employed to localize a target [2].

In this context, researchers and the industry propose to experimentally evaluate, several signal metrics and technologies in the RF domain. Five signal metrics can be leveraged to extract the user position and will be analyzed in Section II-A: RSS, Time of Flight (ToF), Channel State Information (CSI), Channel Impulse Response (CIR), and AoA.

A. Survey on Positioning

In this section, we make a review of the most used signal metrics exploited for indoor localization purposes, by analyzing papers from Scopus digital library up to 2023. The 17 880 surveying scientific papers have been selected, by restricting only to those papers related to RF technologies applied to indoor localization systems.[1] With this analysis, we aim to provide an overview of the volume of papers related to this domain. To achieve this, we specifically focused on papers with title, abstract, or keywords explicitly referred to indoor localization. Fig. 1 shows how signal metrics are combined with the RF technologies and positioning methods in the literature. In particular, we aim to provide a qualitative understanding that papers on BLE with AoA (the same technology and signal metrics of our study) are relatively scarce compared to the overall works in the literature. Therefore, in this section we concentrate on signal metrics to demonstrate which signals are more extensively investigated.

The RSS technique is one of the simplest and widely adopted metric for indoor localization, as RSS is available in all wireless

[1]TITLE-ABS-KEY (((in*door PRE/3 (loca*tion OR positioning OR navigation*)) OR (in*door AND (((position* OR loca*tion) PRE/0 accuracy) OR "simultaneous loca*tion and mapping" OR lbs OR (location PRE/0 (aware OR based) PRE/0 (service* OR system*)) OR fingerprint* OR "received signal strength")))) AND DOCTYPE (cp OR ar) AND SRCTYPE (p OR j) AND SUBJAREA (comp OR engi) AND LANGUAGE (english) AND NOT (TITLE (robot*) OR KEY (robot*))

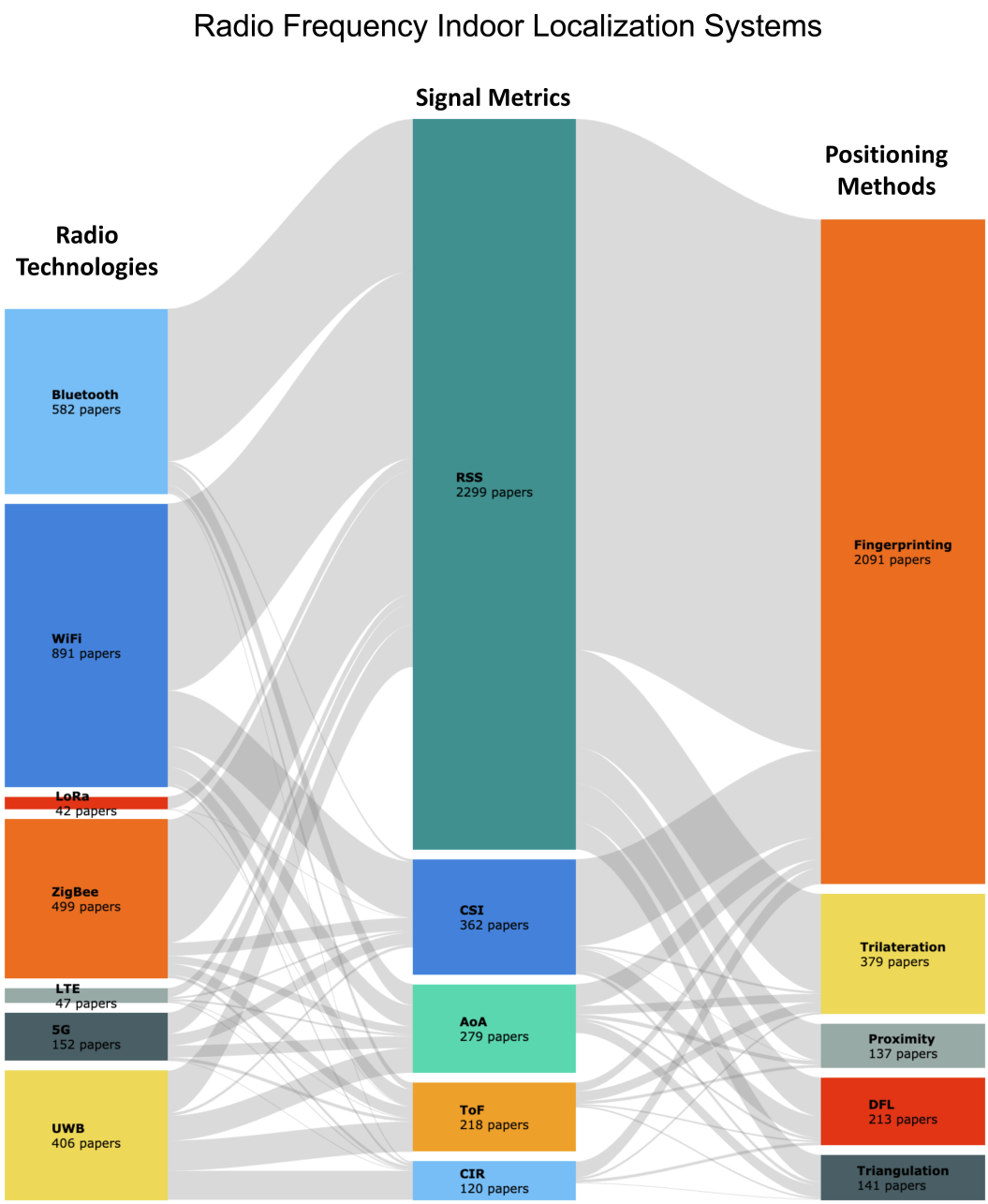

Fig. 1. Alluvial diagram showing the relationship between radio technologies, signal metrics, and positioning method (DFL stands for device-free localization). The data were extracted from the Scopus digital library up to 2023.

technologies and it does not require any specific hardware. RSS measures the signal power strength received at the receiver, measured in decibel-milliwatts (dBm). Moreover, RSS can be used to estimate the distance between transmitter (Tx) and receiver (Rx) devices; reasonably the higher the RSS value, the smaller the distance between the devices. The resulting distance can be estimated with a number of signal propagation models [8], [9] given that the transmission power or the power at a reference point is known. RSSI (which is often confused with RSS) is the RSS indicator, a relative measurement of the RSS that has arbitrary units proposed by each chipset vendor. The RSS metric merely provides the estimated average amplitude over the whole signal bandwidth accumulating signal over all antennas, if any. Therefore, RSS is susceptible to multipath effects and interference that produce high variability over time. The channel state information (CSI) is the subcarrier-level channel measurement for each orthogonal frequency division multiplexing (OFDM) subcarrier, measured at the receiver side. CSI provides more extended multipath information and more stable measurements. For this reason, it can be used to improve the localization accuracy. A different approach is obtained with the channel impulse response (CIR), which measures the power delay profile. In practice, in a multipath channel, the CIR value reveals information about the propagation delay of each path. It

is worth to notice that both CSI and CIR techniques represent signal metrics, which are more robust to multipath effect and to indoor environmental noise. However, they are not easily available with commercial devices.

Time of Flight (ToF) leverages the signal propagation time to calculate the distance between a transmitter and a receiver. The underlying idea is relatively simple, the distance between the emitter and the receiver can be obtained by multiplying the estimated ToF with the speed light (which is constant value k). Although the ToF technique requires a strict synchronization process between transmitters and receivers. Indeed, the key aspect affecting the ToF accuracy is the signal bandwidth and the sampling rate. A low sampling rate (in time) reduces the ToF resolution, since the estimated distance may be possible between the sampled intervals. Furthermore, in multipath indoor environments, the larger the bandwidth, the higher the resolution of ToF estimation. Although large bandwidth technologies improve the performance of ToF, they still cannot eliminate the localization error in no-light-of-sight conditions. Indeed, obstacles refract the emitted signals that, traversing through a longer path, increase the estimated ToF. In order to relax the synchronization requirement, the time difference of arrival (TDoA) technique is used. TDoA exploits the difference in signal propagation times from different transmitters, measured at the receiver. Therefore and differently from ToF techniques, where synchronization is needed between the receiver and the transmitter, with the TDoA techniques only synchronization between the transmitters is required.

Angle of Arrival (AoA) measures the angle at which the transmitted signal arrives at the receiver, by estimating the TDoA at each receiver antenna. An insightful analysis of the AoA signal metric when the BT5.1 DF is used will be given in Section III and also discussed in [10]. The main advantage of AoA is that the estimated user position is possible with two anchors in a 2-D environment. Although AoA can provide accurate estimation when transmitter and receiver are relatively close, its accuracy decreases with the distance. Indeed, a slight error in the AoA evaluation is translated into a relevant error in the actual location estimation [10]. Concerning the AoA technique, in this article, we experimentally evaluate the BT5.1 DF based on the AoA technique. Fig. 1 emphasizes that this domain has relatively few works in the literature compared to the wide field of indoor localization research. In the next section, we only focus on papers that explore the BT5.1 DF in real-world experimental settings.

B. Positioning Through the DF Specification

In this section, we provide a review of the state-of-the-art concerning the adoption of AoA with BT5.1 to localize targets in indoor environments.[2] To the best of our knowledge, only few works are based on real-word experimental settings, while the majority of published works rely on simulated scenarios or on the AoA estimation algorithms. Cominelli et al. [11] presented a scenario with two fixed receiver anchors, based on software defined radios (SDR) reproducing the packets constant tone extension CTE (more details concerning the use of CTE are reported in Section III). The solution proposed by the authors calculates the beacon position taking into account both the AoA of the received packets and the spatial position of the receiving antennas. Authors found that as the frequency of the used channels increases, the AoA average absolute error decreases. In the indoor settings, the absolute AoA error is contained within 5° considering the 15° to 90° range, while the positioning errors are below 85 cm for more than 95% of the tested positions. In [12], Pau et al. presented an hybrid solution, based on the SLWSTK6006A[3] kit. The kit adopts both the AoA and the RSSI obtained from the Bluetooth signal to evaluate the transmitter's location. The experiment, carried out in a real scenario of 25 × 15 m laboratory with four receiving anchors, obtained an average submeter error of 70 cm computed on eight locations.

Furthermore, Sambu et al. [13] tested the BOOSTXL-AOA kit to estimate the AoA and positioning errors in both indoor and outdoor environments. Tests conducted in indoor environments are performed with two anchors in a room of 20 × 25 m with several obstacles such as walls, desks, tables, and standing light. The computed average angular error, for angles between 15° and 90°, is 1.83°. The positioning error, computed on a smaller 5 × 5 2 m-spaced locations grid, is 36.5 cm. The previously mentioned works do not study in depth the impact of body attenuation on the localization process. In [14], Babakhani et al. evaluated only the angular error (no discussion about localization error) in a 8 × 8 m environment. The anchor node is deployed on a tripod and some obstacles are present in the environment, such as pillars, walls, desks, tables, etc. Authors proposed a recurrent neural network to estimate the AoA measuring an average angular error of 7.1°. The main issue of this work is the experimental setting. Indeed, the user did not stay in a fixed position, rather she moved in the environment (the velocity is unknown) in an unknown path. The ground truth is obtained by deploying four Ultra-Wideband (UWB) anchors in the environment. However, no clear information is provided concerning the process required to obtain the ground truth. Under this respect, we refer to [15], [16] as guidelines to design a consistent and accurate process for collecting ground truth locations. The results presented in [14] showed the performance differences between the estimated positions of two systems (BLE-AoA and UWB-ToF) and not the performance of an AoA-based system with respect to a reference system.

Pan and Ho [17] evaluated the performance in an outdoor environment of the localization error. They measured a localization error of 22 cm but in just one position, which is not sufficient to draw a general conclusion for indoor environments. Ye et al. [18] experimentally evaluated the performance in terms of localization error of the Nordic AoA kit. The positioning

[2]TITLE-ABS-KEY (((ble OR bluetooth) AND (aoa OR (angle PRE/0 of PRE/0 arrival))) AND ((in*door PRE/3 (loca*tion OR positioning OR navigation*)) OR (in*door AND (((position* OR loca*tion) PRE/0 accuracy) OR "simultaneous loca*tion and mapping" OR lbs OR (location PRE/0 (aware OR based) PRE/0 (service* OR system*)) OR fingerprint* OR "received signal strength")))) AND DOCTYPE (cp OR ar) AND SRCTYPE (p OR j) AND SUBJAREA (comp OR engi) AND LANGUAGE (english) AND NOT (TITLE (robot*) OR KEY (robot*))

[3][Online]. Available: https://www.silabs.com/development-tools/wireless/efr32xg21-wireless-starter-kit

TABLE I
SUMMARY OF BT5.1 EXPERIMENTS BASED ON A REAL-WORLD SETTING

Work	HW/SW	n° of anchors	Posture	Env. [m]	eval. points	AoA error [°]	loc. error [m]	Scenario
[11]	SW (SDR)	2	N.A.	6x3	20	5	0.85	static
[12]	HW (SLWSTK6006A)	4	N.A.	25x15	8	N.A.	0.7	static
[13]	HW (BOOSTXL-AOA)	2	N.A.	5x5	4	1.83	0.365	static
[14]	HW (XPLR-AOA-1)	1	N.A.	8x8	N.A.	7.1	N.A.	mobility
[17]	HW (BOOSTXL-AOA)	1	N.A.	outdoor	1	N.A.	0.22	static
[18]	HW (NRF52833)	1	N.A.	4.8x4.8	49	5	0.7	static
[19]	SW (SDR)	1	N.A.	N.A.	10	≈ 2	N.A.	static
[20]	HW (UCA-8 Array)	1	N.A.	5.6x4.5	1	≈ 15.8	≈ 1.16	static
[21]	HW (BG22-RB4191A)	1-2	N.A.	3x3	49	N.A.	0.29	static
[22]	HW (XPLR-AOA-1)	1	N.A.	7.5x18	N.A.	N.A.	0.27	mobility
[23]	HW (BOOSTXL-AOA)	1-4	N.A.	2x2 4x4	9	N.A.	0.26	static mobility
proposed solution	HW (XPLR-AOA-1)	1	✓	13.8x8	28	5, refer to [10].	1.82	static mobility proximity

error, computed on a smaller 4.8 × 4.8 m area, is 70 cm without taking into account the posture of the user in a static scenario. Additionally, in [19], Toasa et al. measured an angular error of 2° by using SDR hardware in 10 locations. Paulino et al. [20] presented a self-localization system, where a receiver with an antenna array utilizes the AoAs from fixed beacons to self-localize without a centralized system. Concerning the indoor scenario, they achieved a mean error of 1.16 m in position estimations and compute the AoA with an error of about 15.8°. Wan et al. [21] presented an experimental evaluation of their algorithm, deploying at first one anchor and, second, two anchors in an indoor empty environment. They achieved a localization error of 0.29 m with the two-anchors configuration, but they consider only the static scenario, without the impact of the human body. In [22] a mobile robot, equipped with a receiving BT anchor, has to track an emitting target object. The robot freely navigates through the indoor environment since a prefixed path to follow is not considered. Authors implemented parallax and vector position calculations from both AoA and RSSI data. Finally, Mustafa et al. [23] presented an indoor positioning and navigation system by using up to four anchors for static and mobility scenarios. They achieved a mean localization error of 0.26 m, limiting two empty areas of 4 and 16m^2, respectively. Also in this work, the system does not contemplate the impact and the orientation of the human body. Table I summarizes a selection of recent works, reporting.

1) The number of deployed anchor nodes.
2) If the work considers the user's orientation.
3) Features of the environment.
4) The number of evaluation points.
5) Average AoA error.
6) The obtained localization error.
7) The scenario taken into account.

The previously described papers reveal the need to further investigate the potentialities of the AoA technique applied to indoor settings. Our work distinguishes from the existing results for two aspects: the considered scenario and the experimental settings. Concerning the first aspect, we propose a more heterogeneous set of application scenarios, which include static positioning, mobility, and proximity. The combination of them allows us to stress the adopted kit and the proposed algorithm at very different conditions. Furthermore, we include three common scenarios typically adopted in the field of indoor localization. Not only that, but to the best of our knowledge, the majority of works based on Bluetooth 4.x technology focuses on evaluating the impact of the body's orientation on signal propagation [24], [25], [26], [27]. Whereas, Mavilia et al. [28] investigated the impact of body orientation in a static scenario with anchors placed on the wall.

Fig. 2. Bluetooth packet format supporting DF capability.

Differently from the reviewed papers, our work goes beyond by measuring localization errors in a more heterogeneous set of application scenarios, particularly when anchors are placed on the ceiling. Additionally, we aim to describe the impact of four different body orientations on AoA estimation using a BT5.1-compliant hardware kit.

Concerning the second aspect, we test our scenario in a wide indoor environment of about 110 m^2. As reported in Table I, most of the reviewed papers test their solutions in small environments, in which it is not easy to stress the AoA estimations with corner-case conditions. As detailed in Section V, we test our algorithm with angles on the azimuth plane ϕ in the range: $-70° \leqslant \phi \leqslant -70°$.

III. BLUETOOTH 5.1 DF

With the official release of Bluetooth Core Specification v5.1 in 2019, DF has been added to the specification, which can help devices to evaluate the direction of Bluetooth signals. In order to support the DF capability, a transmitter sends BLE protocol data units (PDUs) with a CTE (a RF sinusoidal signal modulated by a series of consecutive ones) that follows the CRC code, as shown in Fig. 2. This signal is received by an array antenna that, estimating the phase difference among the received

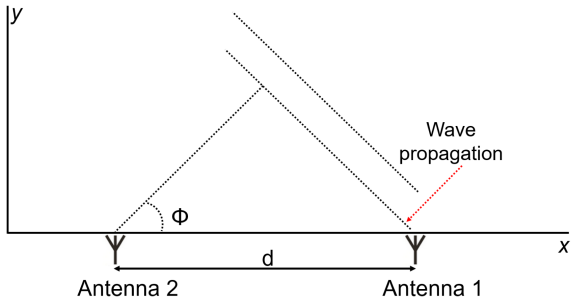

Fig. 3. AoA computation based on the geometry of the antenna array.

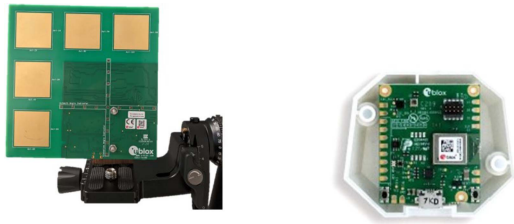

Fig. 4. Hardware kit used for the data collection: Anchor on the left, tag on the right.

signal in each antenna, evaluates the AoA [12]. Conversely, when the antenna array is connected to the transmitter, the system is called AoD. In particular, AoA can be obtained by measuring the phase difference δ between signals received at each pair of neighboring antennas, as the wavelength of the signal λ and the geometry of the antenna, such as the distance d, are known.

Generally, it is possible to consider two angles for estimating the AoA between an anchor and a tag, namely the azimuth ϕ and elevation γ angles. Given a Cartesian plane, the azimuth refers to the angle on the XY plane (azimuth plane), while the elevation angle is computed on a plane orthogonal to the azimuth plane and crossing through the Z-axis. More specifically, given ϕ the estimated AoA on the azimuth plane, it can be obtained as follows: $\phi = \arccos(\frac{\lambda\delta}{2\pi d})$, as reported in Fig. 3. The figure shows two antennas at distance d, and the wavefront propagating from the right-side with angle θ with respect to the antenna's reference plane. The receiver node equipped with an antenna array can, therefore, collect In-Phase and Quadrature (IQ) samples of the signal for every array's antenna. Ultimately, based on the IQ samples, the anchor derives essential details about the received signal, including characteristics like wavelength and frequency. Subsequently, it utilizes this information to calculate the AoA on both the azimuth and elevation.

IV. Experimental Settings

We now detail how we conducted our experimental data collection campaign. Section IV-A details the adopted hardware and the relative configuration settings. Our experiments are based on three application scenarios, identified to test three common situations for humans in indoor environments, namely static positioning, mobility, and proximity. The collected dataset is analyzed in Section IV-C, in which we study some features of the RSSI and AoA values. In particular, we investigate the impact of the Bluetooth communication channels and the impact of different postures for both RSSI and AoA samples.

A. Hardware Kit

The dataset analyzed for this article has been collected with the XPLR-AOA kit produced by u-Blox. The kit is composed by a set of anchor nodes and tag nodes, both supporting the Bluetooth 5.1 DF specification. Anchor's layout is 11.5×11.5 cm board provisioned with an array of five square-shape C211 dual-polarized antennas and powered with the NINA-B4111 BLE module. The anchor node can be also plugged with a Raspberry PI board, through the I/O pins. Tags are equipped with the NINA-B4062 BLE module, they can be configured to vary the advertisement frequency and the power of emission. In particular, we experience with frequencies varying in the range [1, 10, 50] Hz and powers of emission ranging in [−40, +8] dBm. Fig. 4 shows the adopted hardware kit.

Anchor nodes are configured with the u-Blox firmware, namely *u-connectLocate*[4] firmware version 1.0.1, designed to estimate the AoA values for the azimuth and elevation angles, and the RSS of two polarizations expressed in decibel. For more details about AoA estimation, please refer to [14], [29], [30]. The data collected are the following.

1) Azimuth angle ϕ, with $-90° \leq \phi \leq 90°$: The AoA of the current tag's signal in the azimuth plane.
2) Elevation angle γ, with $-90° \leq \gamma \leq 90°$: The AoA of the current tag's signal in a plane orthogonal to the azimuth plane.
3) RSS values of the first and second polarization.
4) The advertisement channel used by the tag (37, 38, 39).
5) The timestamp tracking the uptime of the logging node.

Every anchor estimates the previously described values for each of the collected Bluetooth beacons emitted by a tag. Our experiments are configured with a data rate of 50 Hz, resulting in 3000 expected samples per minute.

B. Experimental Scenarios

Our experiments are conducted in a wide open room located in our research institute. The room's layout is 13.8 × 8 m, covering an area of 110 m^2, the ceiling is 3.1 m high, and no obstacles are present inside the room. The floor is characterized by regular 60 × 60 cm tiles, this layout eases the identification of target locations.

We consider three application scenarios, identified to reproduce indoor real-world situations for humans and to test the hardware and the proposed localization algorithm at different conditions. For all the scenarios, we deploy one anchor node on the ceiling, parallel with respect to the floor. More specifically, we position the anchor with the antenna array oriented toward the floor. The anchor is positioned approximately on the room

[4][Online]. Available: https://www.u-blox.com/en/product/u-connectlocate

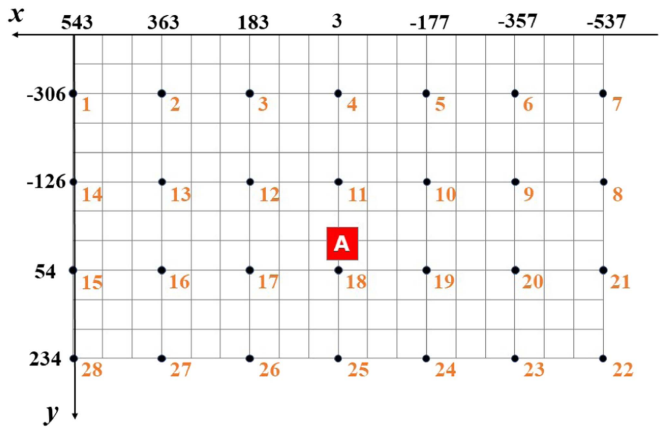

Fig. 5. static positioning scenario. The figure reports the 28 locations and the anchor's position in red.

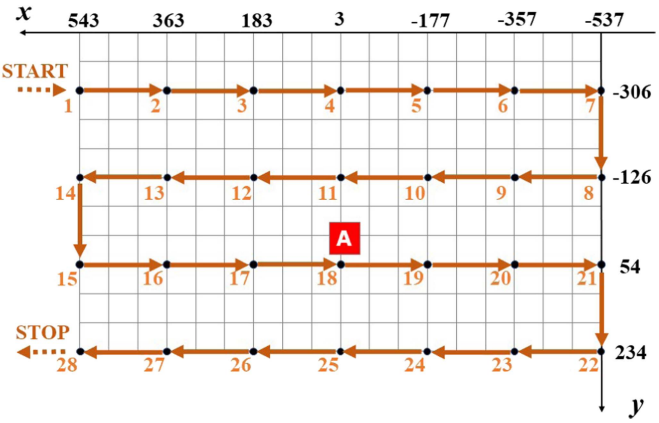

Fig. 6. Mobility scenario. The figure reports the testing path and the anchor's position.

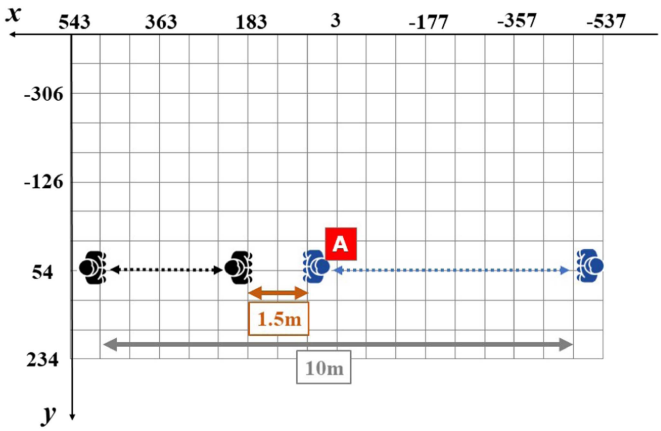

Fig. 7. Proximity scenario. The figure shows the proximity and non-proximity events and the anchor's position.

center, at $z = 3.1$ m from the ground. The tag is held by a person (or two people for the proximity scenario), locked on a lanyard around the neck. The considered scenarios are described in the following.

Static positioning: The goal of this scenario is identifying the location of a person resting in a specific location. More specifically, the person steps over 28 locations on the ground, resting for 2' min in the same position, as shown in Fig. 5. We also vary the posture of the person. In particular, we collect data with the body oriented toward North, East, West, and South, each postures shifts of 90°, so that to evaluate the impact of the body to the collected values. For each of the 28 locations, we expect to collect about 6000 samples (the tag advertises at 50 Hz). From our experiments, we observe a beacon loss rate lower than 10–15%. We execute four runs for this scenario.

Mobility: This scenario reproduces an indoor path. To this purpose, we recruit four different people testing the path with a regular step of, approximately, 0.6 m/s. The path follows a sequence of markers on the ground, and volunteers move in a natural way. Under this respect, it is worth to notice the guidelines proposed by the IPIN Competition (former known as EvaAAL competition) [15], [16], according to which the actor for an indoor localization system should act as natural as possible, by avoiding any bias affecting the overall performance. Each person executes three runs, for a total of 12 runs for this scenario. We report in Fig. 6 the testing path for the mobility scenario.

Proximity: This scenario mimics social interactions between people. With the term interaction, we refer to situations in which the relative distance between two people fits within a specific range. More specifically, we refer to the social distances proposed by Hall [31], according to which four spaces surround a person: intimate, personal, social, and public spaces. Therefore, we include in this article also a proximity scenario whose goal is to detect proximity and nonproximity among people in indoor spaces. The proximity event is obtained with people at [0–2.5]m distance for 2 min, while during nonproximity events people move away at 10 m distance for 2 min. We position on the ground two markers identifying the correct distances. We recruit a pair of volunteers reproducing this scenario, they reproduce three runs each composed by five proximity and five nonproximity events. Fig. 7 shows the proximity scenario.

C. Analysis of the Dataset

We now analyze the collected dataset with the goal of studying how RSSI and AoA values vary. More specifically, we focus on data collected with the static positioning scenario (see Section IV-B), as our goal is to study aspects: The impact of the Bluetooth channels used for advertising and the impact of the body posture at static conditions.

For what concerns the RSSI values, we initially show the density distributions on first and second polarization, as shown in Fig. 8. The matrix reports the 28 locations, according to the layout shown in Fig. 5. In particular, each plot corresponds to the RSSI distribution on the first and the second polarization for the corresponding location. The matrix compares the RSSI distributions on two polarizations, so that to easily spot those locations whose distributions significantly shift. From the figure, we observe some locations where the RSSI estimated on first

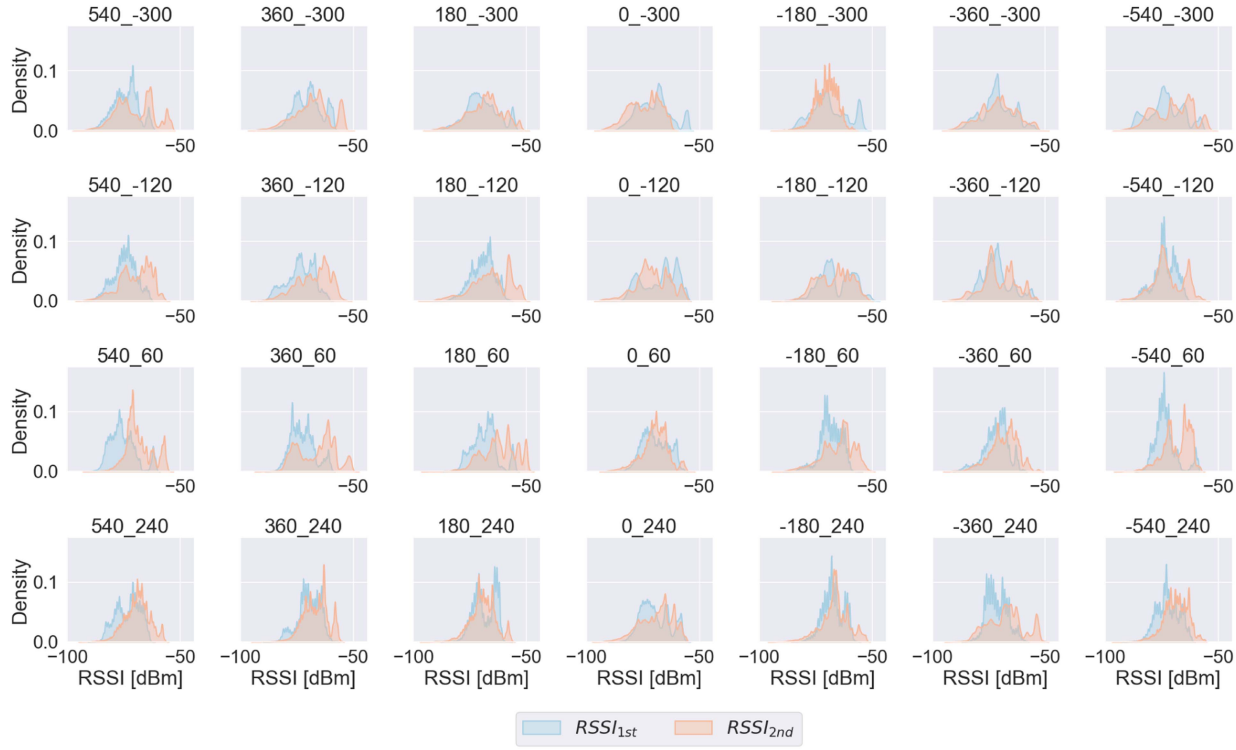

Fig. 8. RSSI distribution on first and second polarization for 28 locations.

polarization remarkably differ from those estimated on second polarization. For instance, in some cases, the angle distributions exhibit patterns like $(-180, 240)$, $(-540, 120)$, $(-360, 120)$, whereas for different locations, the distributions deviate. A discernible recursive pattern that elucidates these variations is elusive. However, it is noteworthy that the Pearson correlation coefficient (ρ) between RSSI values on the first and second polarization is 0.56, signifying a moderate positive correlation.

In order to quantitatively measure the existing correlation between $\text{RSSI}_{1\text{st}}$ and $\text{RSSI}_{2\text{nd}}$, we show in Fig. 9 the relationship between such quantities. From the figure, we observe a moderate positive correlation, with Pearson coefficient $\rho = 0.56$. Therefore, beacons emitted by a tag are generally estimated with a *similar* RSSI values of different angles.

The results reported in Figs. 8 and 9 are obtained by combining the RSSI values estimated on the three channels. However, the channel used for the message propagation impacts the RSSI value, as also shown with some experimental studies based on commercial devices [32], [33], [34]. As the collected dataset also provides information about the adopted channels, we show if and how the adopted channel affects the RSSI density for the first and second polarization. The results of this analysis are reported in Fig. 10. The figure clearly shows that by increasing the channel, the distributions also shift toward stronger RSSI values. Specifically, based on our experiments, we have observed that channel 39 consistently yields the highest RSSI values for both polarizations. The shapes of the reported distributions are characterized by a number of peaks. This pattern is generated by the considered scenario for this analysis. In particular, we analyze the data collected with the static positioning scenario, in which a person steps over 28 locations resting for 2 min. As a result, for each location we observe a different spike in the distribution.

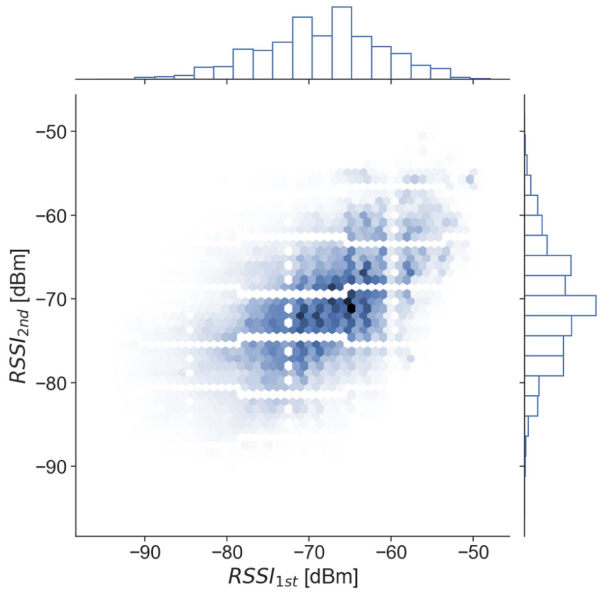

Fig. 9. Correlation between $RSSI_{1st}$ and $RSSI_{2nd}$ on the first and the second polarization.

Table II summarizes median, standard deviation, and max RSSI values for the three channels and the two polarizations.

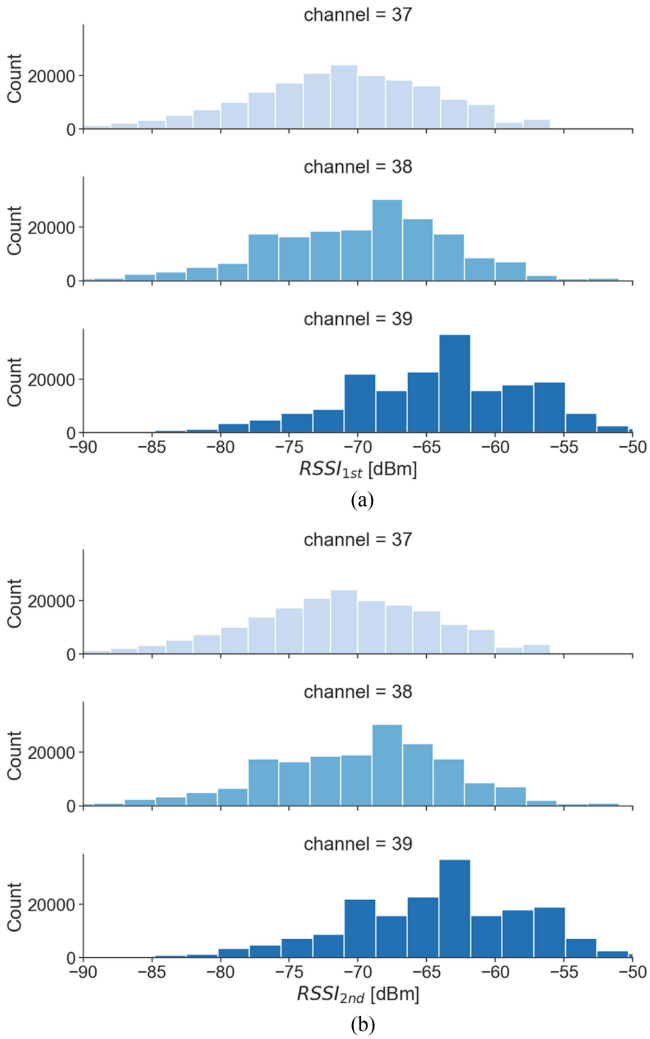

Fig. 10. RSSI distribution for three channels and two polarizations. (a) First polarization. (b) Second polarization.

TABLE II
RSSI STATISTICS FOR THREE CHANNELS AND FOR THE FIRST AND SECOND POLARIZATION

Bluetooth channel	#37	#38	#39
% of collected beacons	33%	32%	33%
μ_{1st} [dBm]	−71.71	−70.03	−64.32
μ_{2nd} [dBm]	−74.16	−72.30	−66.42
σ_{1st} [dBm]	6.74	6.77	6.72
σ_{2nd} [dBm]	5.36	5.30	5.83
max_{1st} [dBm]	−56	−51	−48
max_{2nd} [dBm]	−56	−54	−48

Mean value is represented with μ, standard deviation with σ symbols.

We further analyze the RSSI distribution by evaluating the impact of four different body's orientations combined with three advertisement channels. As detailed in Section IV-B, the static positioning layout has been obtained with four orientations shifting of 90° each. We report in Fig. 11 the corresponding distributions. From the figure, we observe that the different orientations (North, East, West, South) do not significantly alter the trends in the distributions. More specifically, given a polarization, e.g., $RSSI_{1st}$, the three distributions for the three channels follow the same patterns: Channel 39 always provides the strongest RSSI values. We detail in Table III the mean, standard deviation, and max values for the considered variables.

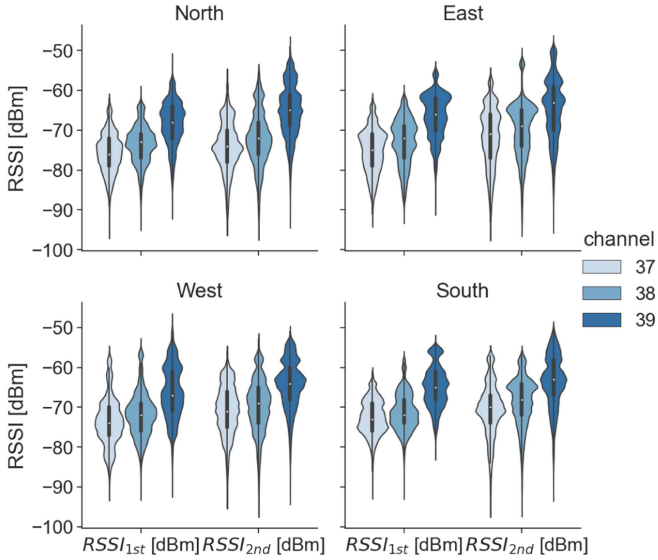

Fig. 11. RSSI distribution on first and second polarization with four orientations (North, East, West, South) and three channels (37, 38, 39).

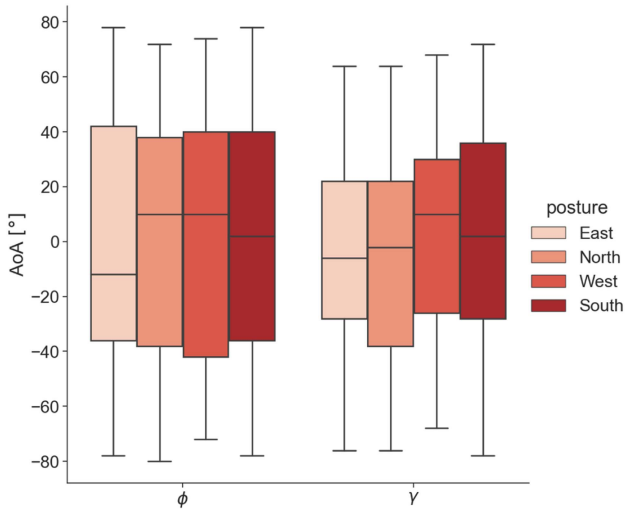

Fig. 12. AoA distribution for different postures and angles.

Finally, we analyze the impact of the body's orientation to the estimated AoA values. For the purpose of this last analysis, we ignore the adopted channel as it does not affect the AoA estimation, as shown in Fig. 12. As expected, the AoA distributions span over a wide range, e.g., from $-70°$ to $70°$, as the plot is obtained by considering all the 28 locations each providing different angle estimations with respect to the anchor's position. From Fig. 12, we observe that orientations have an effect to the AoA values, as shown with the median value represented with an horizontal line for each of the box plots.

TABLE III
STATISTICS FOR THREE ADVERTISEMENT CHANNELS ON 1ST AND 2ND POLARIZATION, RELATIVE TO FOUR ORIENTATIONS

	North			East			West			South		
Channel	37	38	39	37	38	39	37	38	39	37	38	39
μ_{1st} [dBm]	−74	−72.14	−65	−71.6	−69.7	−64.5	−70.6	−69.5	−64.1	−70.5	−68.6	−63.4
μ_{2nd} [dBm]	−75.6	−73.5	−68.2	−75	−72.9	−66.4	−73.4	−71.7	−66.15	−72.4	−71	−64.8
σ_{1st} [dBm]	6.1	6.7	6.4	7.3	7	7.6	6.1	6.6	6	6.6	6.1	6.5
σ_{2nd} [dBm]	4.9	4.7	5.4	5.4	5.7	5.5	6	5.5	6.6	4.2	4.7	5.1
max_{1st} [dBm]	−56	−55	−48	−56	−51	−48	−56	−53	−51	−56	−56	−50
max_{2nd} [dBm]	−62	−60	−52	−62	−60	−54	−56	−54	−48	−61	−57	−53

Mean value of RSS is represented μ, standard deviation with σ symbols.

TABLE IV
STATISTICS FOR THE AZIMUTH ϕ AND ELEVATION γ ANGLES RELATIVE TO FOUR ORIENTATIONS

	North	East	West	South
μ_ϕ [dBm]	0.4	0.83	1.68	0.83
μ_γ [dBm]	−5.6	−3.3	2.149	2.64
σ_ϕ [dBm]	39.8	38.9	40.3	38.3
σ_γ [dBm]	32.8	28.8	30.7	33.6
max_ϕ [dBm]	78	72	74	78
max_γ [dBm]	64	64	68	72

Mean value is represented with μ, standard deviation with σ symbols.

Table IV details the AoA statistic for the different orientations and the AoA angles.

V. EXPERIMENTAL RESULTS

This section details the results we obtain from our data collection campaign. We first detail the process adopted to compute an accurate ground truth, namely the actual location and angle of the reference locations used for the performance assessment with the three scenarios (see Section V-A). We also described the adopted algorithm to compute the location given the estimated AoA values (see Section V-B). Finally, Section V-C details the obtained results.

A. Determining the Location Ground Truth

With the term ground truth (GT), we refer to the actual angles between the target and the anchor nodes. We compute the GT with a geometric approach, detailed in the following.

The GT in the static positioning scenario consists of quadruples of values (x_i, y_i, z_t, o_k), where x and y are the values at position $i = (1 \cdots 28)$ shown with the grid in Fig. 5. The value z_t is the height of the tag, and o_k represents the orientation of the target wearing the tag with $k = \{\text{North, East, West, South}\}$. The quadruple can be converted in two AoA angles of the signal received by the Anchor's antennas $(\omega_i, \gamma_i, o_k)$ corresponding to the expected azimuth angle and elevation angle at position i, for a specific orientation.

Concerning the mobility scenario, the GT is collected in a similar way, by also adding a timestamp tracking the instant in which the target lies in a specific position. In order to record a sufficiently accurate timestamp, the target is equipped with the StepLogger application, also adopted with the IPIN competition [15], [16]. The StepLogger application allows us to record the timestamp (epoch time) and a label, i.e., the identifier of a marker on the ground. In this way, it is possible to rebuild the real location of a target moving indoor. In our case, we position 28 markers on the ground, as reported with the grid in Fig. 6, and for each of them we record the timestamp with the StepLogger application. The expected error for the GT measurement is maximum 20 cm.

Finally, concerning the GT of the proximity scenario, it consists of the timestamp when the pair of targets starts a proximity event and when it starts a nonproximity event. To this purpose and similarly to the previous scenario, we adopt the StepLogger application through which we are able to track the proximity (1.5 m distance) and the nonproximity (10 m away), as reported in Fig. 7.

Similarly to the mobility scenario, the clocks between the anchor node and the StepLogger application are synchronized at the beginning of the experiment. The data collected are therefore a sequence of triples indicating the initial and final time of an interaction and a Boolean variable proximity: (t_i, t_{i+1}, p) with p indicating proximity.

B. Computing the Indoor Location

We implement an indoor localization algorithm able to estimate the target's location for all the tested scenario, in terms of x, y coordinates. The error is calculated as the Euclidean distances from the GT. Concerning the proximity scenario, it represents a classification problem (detecting proximity or nonproximity events). Therefore, given the estimate target's location we compute the interpersonal distance and we compared it against the GT. In the rest of this section, we detail the algorithm used to determine the target's location.

Fig. 13 shows how the azimuth and elevation angles are converted in terms of x, y coordinates. In the experiments the anchor is placed on the ceiling, this means that the azimuth plane is perpendicular to the floor x, y of the room, as shown in Fig. 13(b). To calculate the transformation of the segment $\overline{\text{AT}}$, joining anchor A to the tag, T must be projected on the azimuth plane xz, as shown in Fig. 13(a). The tangent of the azimuth angle ϕ is given by the ratio of two catheti of length x_T and $(z_A - z_T)$, respectively, where z_A is the height of the anchor and z_T the height of the tag. By setting $h = (z_A - z_T)$, the difference in height between anchor and tag, we can write

$$x_T = h \cdot \tan(\phi). \tag{1}$$

The tangent of the elevation angle γ is obtained from the ratio of two other catheti: The first is the projection of the segment $\overline{\text{AT}}$ on the xz plane (colored red), whose length is given by $\sqrt{x_T^2 + h^2}$ and the second one perpendicular to the xz plane and of length

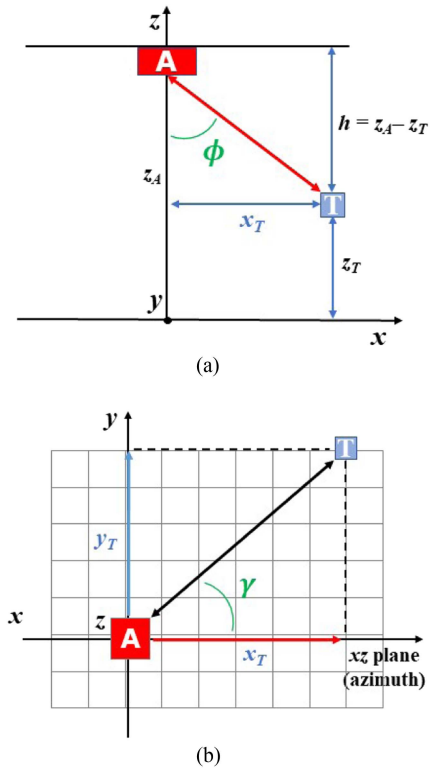

Fig. 13. Geometric representation of ϕ and γ angles. (a) xz plane (vertical plane) (b) xy plane.

y_T: $\tan(\gamma) = y_T/\sqrt{x_T^2 + h^2}$, substituting (1) in this expression we obtain

$$y_T = h \cdot \sqrt{1 + \tan^2(\phi)} \cdot \tan(\gamma) = \frac{h}{\cos(\phi)} \cdot \tan(\gamma). \quad (2)$$

From (1) and (2), we can easily obtain the GT for the static positioning scenario in terms of AoAs. In the mobility scenario, a window of 500 ms was considered to average the measured angles before converting them into positions. While in the proximity scenario all the measures taken in the time interval were considered.

C. Analysis of the Results

We now detail the experimental results obtained for the three scenarios, namely static positioning, mobility, and proximity.

Concerning the static positioning, we compute the error for each of the 28 locations as reported in Fig. 14. The figure reports as white dots the 28 locations and with a red box the anchor's locations (the $(0, 0)$ coordinate). We report the results for the four orientation (North, East, West, and South) and for each plot, we report the coordinates both on the x, y axis. From the figure, we observe that the location error varies not only according to the locations, but also according to the posture. As a general trend, we observe that locations *close* to the anchor node result with the lowest errors, while locations on the peripheral areas (e.g., upper/lower left/right corners) tend to increase the errors.

From Fig. 14, we also observe that the orientation affects the low-error region. With the North orientation, the low-error region is evenly centered around the anchor's location, with a mean error of 1.90 m. With the East orientation, such regions are shifted to values of $x = [183 - 3]$. This shift depends from the orientation of the user. In particular, as the user is oriented toward East, the low-error region exists in those location in which the user is in line-of-sight with the anchor. As soon as the anchor is behind the user, e.g., locations $(-177, 54)$, the error tends to increase. The mean error obtained with the East orientation is 1.90 m. Similarly, the low-error region with the West orientation is centered in location $(-177, -128)$. As soon as the user is ahead the anchor's location, the error tends to increase, in this case the mean error is 1.82 m. Similar considerations apply also for the South orientation with a mean error of 1.88 m. Results concerning the mobility scenario are reported in Fig. 15. The figure shows the path followed by the target and, for each of the 28 path's locations, we report: The ground truth, the estimated location, and the error as a black line. We execute 12 runs for the mobility scenario, and Fig. 15 reports the mean localization error for all the runs. From the figure, we can distinguish two behaviors. First, locations far from the anchor's position generally result with higher localization errors with respect to locations close to the anchor. This aspect can be observed by considering the error bars, which increase with the peripheral locations, and decrease with locations surrounding the anchor. Second, the implemented algorithm tends to *attract* the target toward the anchor's locations. The attraction effect remains consistent in the static scenario as well. In Fig. 14, the most significant errors are identified along the perimeter of the room, particularly pronounced on the sides farther from the anchor. This is due to the fact that, with the same angular error, the error in meters is amplified for locations that are more distant.

The maximum and minimum localization errors correspond to 4.8 and 0.11 m, respectively, with a mean value of 1.83 m and a median error of 1.55 m. According to the framework adopted with the IPIN Competition [2], [15], [16], we also compute the 75th percentile, as it represents a robust statistic mitigating the effect of outlier estimations. From our experiment, the 75th percentile of the error corresponds to 2.78 m. We further investigate the error distribution, and we plot the cumulative distribution function (CDF) in Fig. 17.

Similar considerations also apply for the best and worst runs, which are reported Fig. 16. The best run represents the run in which we measure the lowest locations error, with a mean error of 1.74 m and 75th percentile of 2.97 m. Concerning the worst run, the corresponding mean error is 1.94 m and 75th percentile 2.94 m.

Concerning the proximity scenario, we execute our algorithm with the goal of identifying proximity and nonproximity events. As reported in Fig. 7, two targets are in proximity at 1.5 m distance for 2 min and then they are in nonproximity when they move away for 2 min. We test the algorithm by varying the distance threshold τ. Such threshold models the minimum distance at which an interaction between the targets starts. In particular, we test values of τ ranging from 1.5 to 4 m, whose results are shown in Fig. 18. As τ increases, our algorithm tends to also increase the false positive rate (the algorithm classifies proximity against a nonproximity event), as shown with the

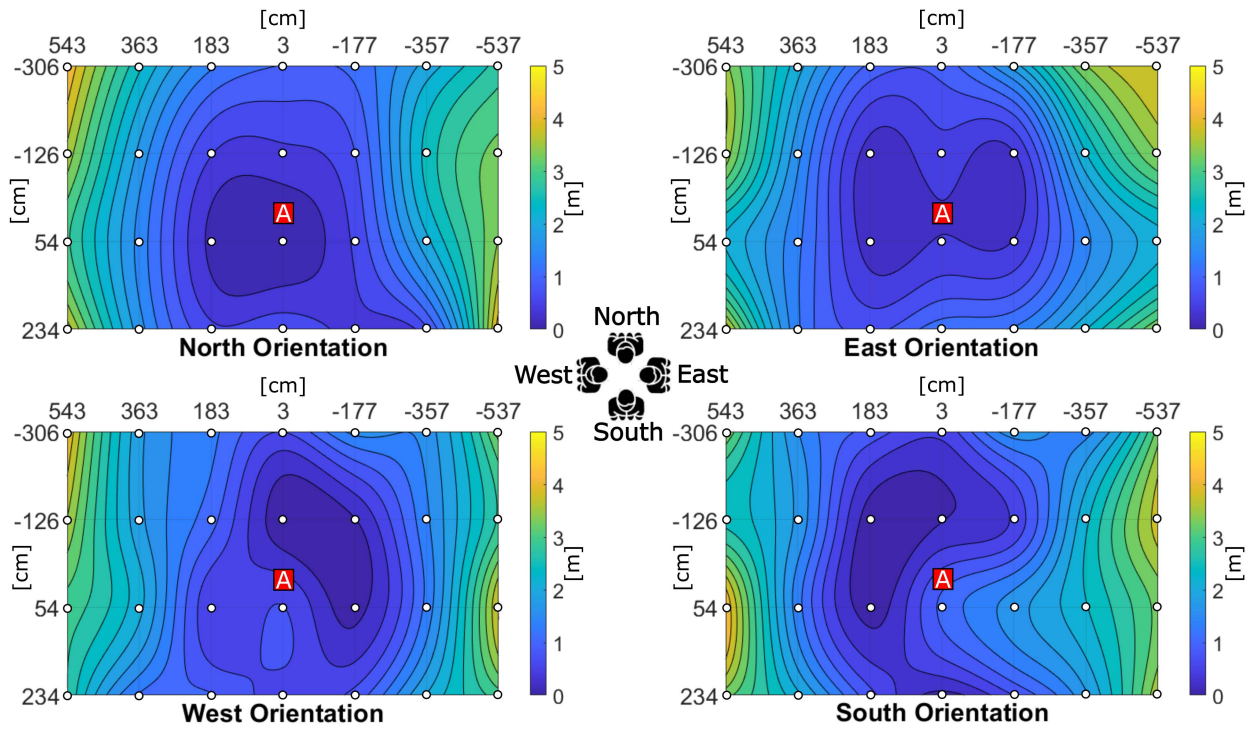

Fig. 14. Experimental results for the static positioning scenario: The contour maps show the localization error for each of the 28 locations and the four orientations.

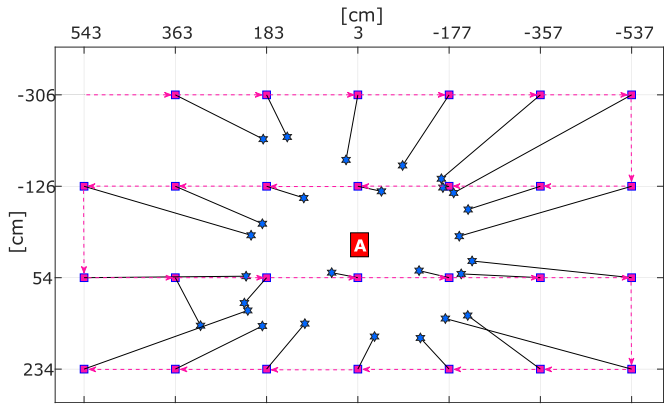

Fig. 15. Experimental results for the mobility scenario: For each of the locations along the path, the graph shows the ground truth locations (as purple boxes) and the estimated locations (as blue stars). Black lines measure the locations errors. Anchor's locations are denoted with a red box.

precision metric. Such curve starts decreasing at $\tau = 2.5$ m distance, meaning that after such distance the algorithm wrongly classifies nonproximity events. Conversely, the accuracy and F-Score metrics increase up to $\tau = 3.5$ m, after which the algorithm wrongly classifies the proximity events. For the purpose of this work, we set the $\tau = 2.5$ m, and we report in Table V the obtained results. In particular, the algorithm classifies proximity with 93.81% accuracy and 93.11% F-Score. It is important to acknowledge that the proximity test was conducted in close proximity to the anchor location. It remains uncertain whether

TABLE V
CONFUSION MATRIX AND METRIC RESULTS FOR THE PROXIMITY SCENARIO AND DISTANCE THRESHOLD SET TO 2.5 m

	Expected Results		accuracy [%]	F-Score [%]
	proximity	Non-proximity		
proximity Events	3304	39	93.81	93.11
Non-proximity Events	450	4104		

comparable performance can be achieved with a test conducted in the peripheral area of the room, where, as previously mentioned, positions are drawn toward the anchor. However, proximity measures are relative and not absolute distances. Therefore, if both individuals in proximity are positioned at the room's edge, both their positions should be influenced by the anchor, preserving the relative distance. Naturally, this consideration warrants validation through additional experiments, as there is a possibility that one person could overshadow the other.

VI. CONCLUSION

Indoor localization systems have gained an increasing attention, as they open to the possibility of improving the usability of a wide plethora of services target to end-users, also referred to as location-based services (LBS).

Differently from the outdoor scenarios in which GNSS-based solutions are well consolidated, indoor environments still represent a challenging scenario. Under this respect, it is worth to mention the existence of several indoor localization competitions (e.g., IPIN [16], TC4TL [35], Indoor Localization Competition 2.0 [36]), which aim at testing and compare state-of-the-art techniques with real-wold settings. A multitude of techniques

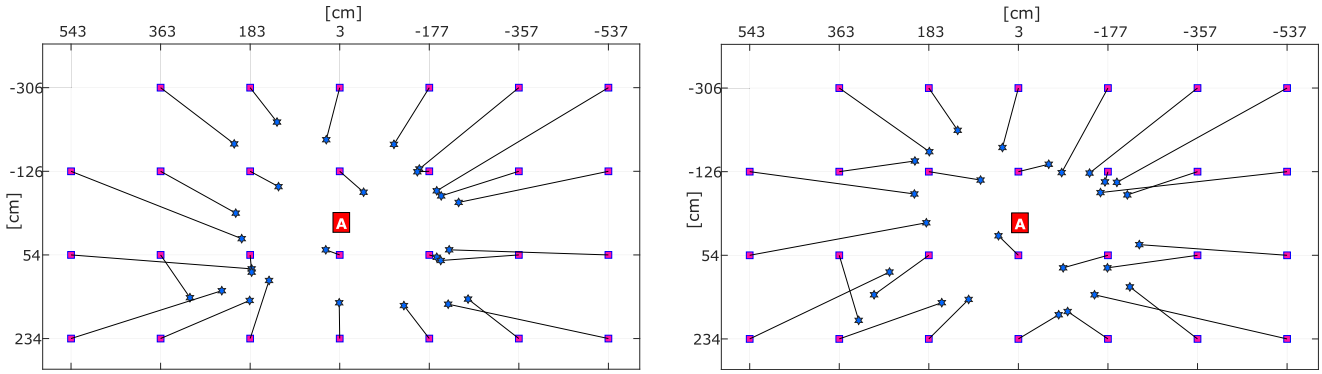

Fig. 16. Experimental results for the mobility scenario concerning the best (left-side) and worst run (right-side).

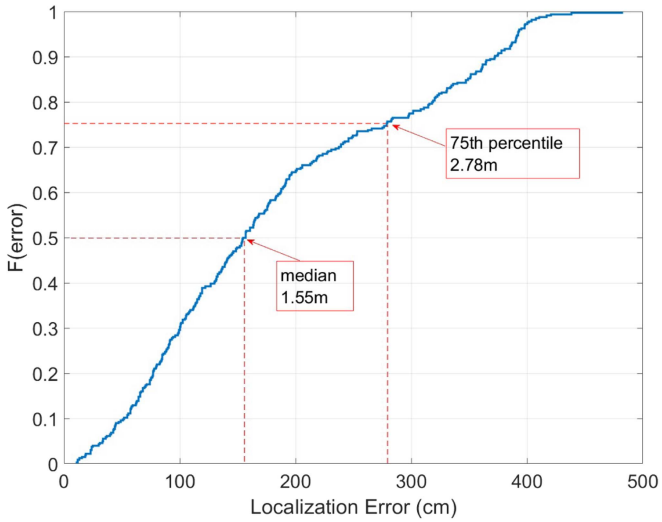

Fig. 17. Cumulative distribution function of the localization error for the mobility scenario.

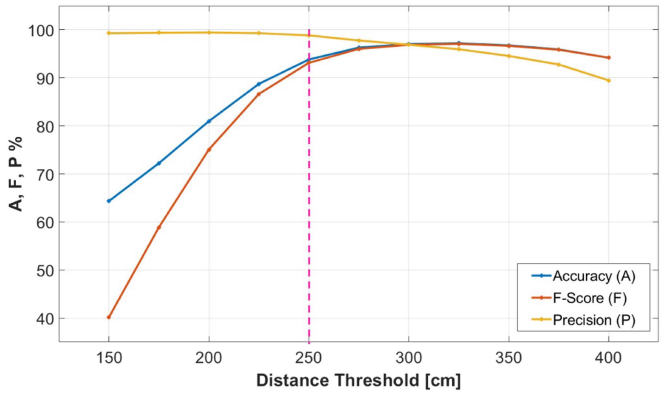

Fig. 18. Experimental results for the proximity scenario: The graph shows the accuracy (A), F-Score (F), and precision (P) by varying the distance threshold.

can be adopted to localize a target indoor, ranging from visible light, ultrasound, acoustic signals and radio-frequency (RF) techniques. Among them, the family of RF-based approaches traditionally has successfully demonstrated the possibility of localizing a target indoor. In this work, we explored the potentialities of Bluetooth 5.1 DF specification based on AoA estimations. We define three localization scenarios, static positioning, mobility, and proximity and we evaluate the performance in terms of the localization error. The considered scenarios cover three reference use-cases commonly experimented in the field of indoor localization. More specifically, we test the proposed algorithm to localize a target resting in 28 locations for two minutes, a moving target following an indoor path and, finally, two targets reproducing a social meeting in proximity (1.5 m distance) and nonproximity. To this purpose, we deploy one anchor node equipped with an antenna array on the ceiling, in a wide open room and we assigned to the target a Bluetooth 5.1 tag held around the neck. From our experiments, we measure the average localization error varying according to the considered scenario. Concerning the static positioning, we measure an average error below 2.1 m, for the mobility scenario the 75th percentile of the localization error is 2.78 m. Finally, the obtained performance for the proximity scenario shows that our solution is able to successfully detect proximity with an accuracy of 94.58%. The availability of data is a crucial aspect that we have thoroughly taken into account. We intend to share the data gathered in this study to facilitate additional research and ensure reproducibility. In this regard, it is worth noting that we have already initiated the publication of data derived from AoA measurements, collected using Bluetooth 5.1 devices. Currently, we have released a dataset featuring information from four anchors as reported in [37].

From the results described in this article, we derive some consideration concerning the use of AoA-based solutions to localize a target. First the orientation of the target affects the overall results. In this work, we experiment with four orientations: North, East, West, and South each shifting of 90° with respect to the anchor's position. As expected and already verified with RSS-based approaches, the effect of the human body is to reduce the signal propagation and, in turn of increasing signal reflections, giving rise to the multi-path effect. Such effects are shown with the heatmaps reported in Fig. 14. A second consideration refers to the anchor's location. In our experimental setting, we

deploy the anchor on the ceiling with the antenna oriented toward the floor. In our previous study [10], we experience with different anchor's deployments, such as anchors deployed on the wall with α° inclination. However, such last deployments increase the complexity to determine the target's location as the anchor's inclination requires a more complex geometric computation.

Furthermore, we observe a decrease of the performance with anchor wall mounted, leading us to prefer a ceiling-mounted anchor. A further consideration refers to the number of required anchors to guarantee a specific performance. More specifically, in this work we only deploy one anchor. We consider as a promising research line to also investigate the possibility of deploying multiple anchors in the same environment (as done in [37]), and to estimate the target's location by jointly considering AoA values from all the anchors. From a preliminary analysis, this approach would increase the performance at a reduced deployment cost. More specifically, we note two pivotal aspects in our observations. 1) The position of the anchor significantly influences the quality of the collected data. 2) The orientation of the anchor not only plays a crucial role in determining the quality of the collected data, but it also influences the ease of installation. Regarding the first aspect, anchors may be positioned according to various layouts, the center of the wall, the corners of the room or on the ceiling. Based on our experience, we observe that the optimal layout strictly depends on the shape of the testing environment. As a general consideration, it is advisable to avoid layouts in which the angle on the azimuth plane between anchors and target exceeds of 70°–80°. Indeed, such angles usually represent the most critical conditions for AoA estimation. As for the second aspect, the orientation of anchors is also pivotal. We experimented with vertical, tilted, and horizontal orientations. The impact is twofold: on one hand, the orientation influences the computation of the target's location, and on the other hand, it can extend the deployment phase. Ensuring uniform orientation for all anchors is essential, and in the case of tilted anchors, replicating the same inclination might pose challenges during installation.

Finally, our last consideration refers to the use of multiple techniques, such as combining RSS and AoA together and a filtering or training strategy to estimate the location. Data-fusion represents the path to pursue to make a significant step toward submeter localization accuracy. In particular, we refer to use of RSS to estimate the distance and, at the same time, to exploit the AoA values to estimate the direction of the signals. Such combination could be processed with filtering techniques, such as Particle filter [38] or Kalman filter [39] in order to attenuate the signal noise and to provide stable results.

REFERENCES

[1] F. Zafari, A. Gkelias, and K. K. Leung, "A survey of indoor localization systems and technologies," *IEEE Commun. Surv. Tut.*, vol. 21, no. 3, pp. 2568–2599, Jul.–Sep. 2019.

[2] F. Potortí, A. Crivello, F. Palumbo, M. Girolami, and P. Barsocchi, "Trends in smartphone-based indoor localisation," in *Proc. Int. Conf. Indoor Positioning Indoor Navigation*, 2021, pp. 1–7.

[3] C.-C. Pu and W.-Y. Chung, "Mitigation of multipath fading effects to improve indoor RSSI performance," *IEEE Sensors J.*, vol. 8, no. 11, pp. 1884–1886, Nov. 2008.

[4] M. R. Basheer and S. Jagannathan, "Localization and tracking of objects using cross-correlation of shadow fading noise," *IEEE Trans. Mobile Comput.*, vol. 13, no. 10, pp. 2293–2305, Oct. 2014.

[5] Y. Zhuang, J. Yang, Y. Li, L. Qi, and N. El-Sheimy, "Smartphone-based indoor localization with bluetooth low energy beacons," *Sensors*, vol. 16, no. 5, 2016, Art. no. 596.

[6] J. Zhang, G. Han, N. Sun, and L. Shu, "Path-loss-based fingerprint localization approach for location-based services in indoor environments," *IEEE Access*, vol. 5, pp. 13756–13769, 2017.

[7] M. Woolley, "Bluetooth direction finding," *Tech. Overview*, 2019.

[8] K. N. R. S. V. Prasad, J. Cheng, and V. K. Bhargava, "Accurate distance estimation for RSS localization with statistical path loss exponent model," in *Proc. IEEE Glob. Commun. Conf.*, 2020, pp. 1–6.

[9] G. Wang and K. Yang, "A new approach to sensor node localization using RSS measurements in wireless sensor networks," *IEEE Trans. Wireless Commun.*, vol. 10, no. 5, pp. 1389–1395, May 2011.

[10] M. Girolami, P. Barsocchi, D. La Rosa, F. Furfari, and F. Mavilia, "Evaluation of angle of arrival in indoor environments with bluetooth 5.1 direction finding," in *Proc. 18th Int. Conf. Wireless Mobile Comput., Netw. Commun.*, 2022, pp. 284–289.

[11] M. Cominelli, P. Patras, and F. Gringoli, "Dead on arrival: An empirical study of the Bluetooth 5.1 positioning system," in *Proc. 13th Int. Workshop Wireless Netw. Testbeds, Exp. Eval. Characterization*, 2019, pp. 13–20.

[12] G. Pau, F. Arena, Y. E. Gebremariam, and I. You, "Bluetooth 5.1: An analysis of direction finding capability for high-precision location services," *Sensors*, vol. 21, no. 11, 2021, Art. no. 3589.

[13] P. Sambu and M. Won, "An experimental study on direction finding of Bluetooth 5.1: Indoor vs outdoor," in *Proc. IEEE Wireless Commun. Netw. Conf.*, 2022, pp. 1934–1939.

[14] P. Babakhani, T. Merk, M. Mahlig, I. Sarris, D. Kalogiros, and P. Karlsson, "Bluetooth direction finding using recurrent neural network," in *Proc. Int. Conf. Indoor Positioning Indoor Navigation*, 2021, pp. 1–7.

[15] F. Potortì et al., "The IPIN 2019 indoor localisation competition—description and results," *IEEE Access*, vol. 8, pp. 206674–206718, 2020.

[16] F. Potortì et al., "Off-line evaluation of indoor positioning systems in different scenarios: The experiences from IPIN 2020 competition," *IEEE Sensors J.*, vol. 22, no. 6, pp. 5011–5054, Mar. 2022.

[17] G. Pan and J. Ho, "Indoor positioning experiments based on BT 5.1," in *Proc. IEEE 4th Int. Conf. Power, Intell. Comput. Syst.*, 2022, pp. 687–692.

[18] H. Ye, B. Yang, Z. Long, and C. Dai, "A method of indoor positioning by signal fitting and PDDA algorithm using BLE AOA device," *IEEE Sensors J.*, vol. 22, no. 8, pp. 7877–7887, Apr. 2022.

[19] F. A. Toasa, L. Tello-Oquendo, C. R. Peñafiel-Ojeda, and G. Cuzco, "Experimental demonstration for indoor localization based on AOA of Bluetooth 5.1 using software defined radio," in *Proc. IEEE 18th Annu. Consum. Commun. Netw. Conf.*, 2021, pp. 1–4.

[20] N. Paulino and L. M. Pessoa, "Self-localization via circular Bluetooth 5.1 antenna array receiver," *IEEE Access*, vol. 11, pp. 365–395, 2023.

[21] Q. Wan et al., "A high precision indoor positioning system of BLE AOA based on ISSS algorithm," *Measurement*, vol. 224, 2023, Art. no. 113801.

[22] K. Weinmann and S. Simske, "Design of Bluetooth 5.1 angle of arrival homing controller for autonomous mobile robot," *Robotics*, vol. 12, no. 4, 2023, Art. no. 115.

[23] A. K. Mustafa and E. R. Sykes, "A high fidelity indoor navigation system using angle of arrival and angle of departure," in *Proc. Work Prog. Papers 13th Int. Conf. Indoor Positioning Indoor Navigation*, 2023.

[24] P. Baronti, M. Girolami, F. Mavilia, F. Palumbo, and G. Luisetto, "On the analysis of human posture for detecting social interactions with wearable devices," in *Proc. IEEE Int. Conf. Hum.- Mach. Syst.*, 2020, pp. 1–6.

[25] M. J. Christoe, J. Yuan, A. Michael, and K. Kalantar-Zadeh, "Bluetooth signal attenuation analysis in human body tissue analogues," *IEEE Access*, vol. 9, pp. 85144–85150, 2021.

[26] M. Shi and L. Kreitzman, "Contact tracing for COVID-19 using Bluetooth low energy," *J. Student Res.*, vol. 11, no. 1, Feb. 2022.

[27] M. Girolami, F. Mavilia, and F. Delmastro, "Sensing social interactions through BLE beacons and commercial mobile devices," *Pervasive Mobile Comput.*, vol. 67, 2020, Art. no. 101198.

[28] F. Mavilia, P. Barsocchi, F. Furfari, D. La Rosa, and M. Girolami, "On the analysis of body orientation for indoor positioning with BLE 5.1 direction finding," in *Proc. IEEE Int. Conf. Commun.*, 2023, pp. 204–209.

[29] I. Gouzouasis, S. Papaharalabos, M. A. Nasa, and P. Karlsson, "A novel antenna system for direction finding applications using BLE 5.1 technology," in *Proc. 17th Eur. Conf. Antennas Propag.*, 2023, pp. 1–5.

[30] M. V. Gamarra, S. Papaharalabos, F. Rezaei, D. Bartlett, and P. Karlsson, "Seamless indoor and outdoor positioning with hybrid bluetooth AOA and GNSS signals," in *Proc. 13th Int. Conf. Indoor Positioning Indoor Navigation*, 2023, pp. 1–6.
[31] E. Hall and C. P. C. L. of Congress, *The Hidden Dimension* (Anchor books. Doubleday Series). New York, NY, USA: Knopf Doubleday Publishing Group 1966. [Online]. Available: https://books.google.it/books?id=zGYPwLj2dCoC
[32] C. Gentner, D. Günther, and P. H. Kindt, "Identifying the BLE advertising channel for reliable distance estimation on smartphones," *IEEE Access*, vol. 10, pp. 9563–9575, 2022.
[33] J. Wilson and N. Patwari, "Radio tomographic imaging with wireless networks," *IEEE Trans. Mobile Comput.*, vol. 9, no. 5, pp. 621–632, May 2010.
[34] P. Barsocchi, M. Girolami, and D. La Rosa, "Detecting proximity with bluetooth low energy beacons for cultural heritage," *Sensors*, vol. 21, no. 21, 2021, Art. no. 7089. [Online]. Available: https://www.mdpi.com/1424-8220/21/21/7089
[35] D. A. R. Seyed Omid Craig S. Sadjadi Greenberg, "NIST pilot too close for too long (TC4TL) challenge evaluation plan," NIST, Tech. Rep., 2020. [Online]. Available: https://www.nist.gov/itl/iad/mig/nist-tc4tl-challenge
[36] Y. Shu, Q. Xu, J. Liu, R. R. Choudhury, N. Trigoni, and V. Bahl, "Indoor location competition 2.0 dataset," Jan. 2021. [Online]. Available: https://www.microsoft.com/en-us/research/publication/indoor-location-competition-2-0-dataset/
[37] M. Girolami, F. Furfari, P. Barsocchi, and F. Mavilia, "A bluetooth 5.1 dataset based on angle of arrival and RSS for indoor localization," *IEEE Access*, vol. 11, pp. 81763–81776, 2023.
[38] Y. Shen, B. Hwang, and J. P. Jeong, "Particle filtering-based indoor positioning system for beacon tag tracking," *IEEE Access*, vol. 8, pp. 226445–226460, 2020.
[39] Y. Zhao, X. Li, Y. Wang, and C.-Z. Xu, "Biased constrained hybrid Kalman filter for range-based indoor localization," *IEEE Sensors J.*, vol. 18, no. 4, pp. 1647–1655, Feb. 2018.

Michele Girolami received the M.Sc. and Ph.D. degrees in computer science from the University of Pisa, Pisa, Italy, in 2007 and 2015, respectively.

He is currently with ISTI-CNR as a Researcher with the Wireless Network Laboratory. He participates to several EU projects and as national research projects. His research interests are mainly focused on indoor localization, proximity detection, pervasive computing and Internet of Things. He also supports the organization of the IPIN competition and he has been serving with several roles for the organization of workshops and international conferences.

Fabio Mavilia received the Graduate degree in electronic engineering from the University of Pisa, Pisa, Italy, in 2012.

As a member of the Wireless Network Laboratory, he currently holds the position of Researcher with the Institute of Information Science and Technologies National Research Council of Italy. His research interests include Internet of Things and Cyber Physical Systems, with a particular focus on Ambient Intelligence. In particular, his work is focused on development of embedded platforms for wireless sensor networks and of algorithms for indoor activity recognition and for indoor localization, by using unobtrusive sensing devices based on radio frequency technologies.

Francesco Furfari received the Ph.D. degree in information engineering from the University of Pisa, Pisa, Italy, in 2009.

He is currently a Researcher with the Information Science and Technologies Institute (ISTI), National Research Council (CNR), Pisa, Italy. He coordinated several European projects on Ambient Assisted Living for ISTI-CNR, and is the Creator of the EvAAL international competition. His research interests include wireless sensor networks, mobile middleware, IoT, and indoor localization.

Paolo Barsocchi received the M.Sc. and Ph.D. degrees in information engineering from the University of Pisa, Pisa, Italy, in 2003 and 2007, respectively.

He is currently a Researcher with the Information Science and Technologies Institute, National Research Council, Pisa, Italy. He has coauthored more than 100 articles published in international journals and conference proceedings. His research interests are mainly focused in the areas of the IoT, cyber-physical systems, indoor localization, and radio channel signal processing. He is also a member of numerous program committees and Editorial Board of international journals, and the Program Chair and the Co-Chair of several conferences.

Open Access funding provided by 'Consiglio Nazionale delle Ricerche-CARI-CARE-ITALY' within the CRUI CARE Agreement